Accepted for publication in Journal of Applied Polymer Science
Published in January 15, 2014
DOI: 10.1002/app.40447

Fracture behavior of boehmite filled polypropylene block copolymer nanocomposites as assessed by the essential work of fracture concept

T. Turcsán[1], L. Mészáros[1*], V. M. Khumalo[2], R Thomann[3] and J. Karger-Kocsis[1,2,4]

[1]*Department of Polymer Engineering, Faculty of Mechanical Engineering, Budapest University of Technology and Economics, Műegyetem rkp. 3., H-1111 Budapest, Hungary*

[2]*Department of Polymer Technology, Faculty of Mechanical Engineering and Built Environment, Tshwane University of Technology, Pretoria, 0001, South Africa*

[3]*Institut für Makromolekulare Chemie und Freiburger Materialforschungszentrum, Albert-Ludwigs-Universität Freiburg, Stefan-Meier-Strasse 31, D-79104 Freiburg, Germany*

[4]*MTA–BME Research Group for Composite Science and Technology, Műegyetem rkp. 3., H-1111 Budapest, Hungary*

*Corresponding author, e-mail: meszaros@pt.bme.hu

Submitted to: Journal of Applied Polymer Science, September, 2013.

Abstract

The essential work of fracture (EWF) method was adapted to determine the fracture toughness of poly(propylene-block-ethylene) (EPBC) based nanocomposites with different amounts (from 0 up to 5 wt.%) of synthetic boehmite alumina (BA). The dispersion of BA in the matrix was studied by transmission and scanning electron microscopies. Agglomerated micronscale along with well dispersed nanoscale BA particles were present in the EPBC matrix. By contrast to the neat EPBC, all nanocomposites failed by unstable necking. Therefore the energy partitioning concept of the EWF was adapted and attention paid to the yielding-related term. Both specific yielding-related essential and non-essential work of fracture parameters increased linearly with the product of the yield stress and elongation at yield derived from static tensile tests.

Keywords: properties and characterization; structure-property relations; thermoplastics; composites

Introduction

The essential work of fracture (EWF) is a popular method to assess the toughness of ductile metals and polymers under plane stress conditions. EWF belongs to the post yield fracture mechanics and successfully competes with the J-integral. The data reduction of both methods results in resistance curves. The major advantage of the EWF method is that the crack propagation is given by the ligament, whereas it has to be determined by suitable techniques in case of the J-integral. According to the EWF theory the total work of fracture (W_f) is the sum of two components: i) the essential work of fracture (W_e), and ii) non-essential or plastic work (W_p):

$$W_f = W_e + W_p \tag{1}$$

The former is needed to create new surface in the inner fracture process zone, whereas the latter is consumed in the outer plastic deformation zone. W_f is calculated from the area of the force-displacement (F-x) curves registered on pre cracked specimens of various ligament (L) lengths. Because the essential and non-essential zones are surface- and volume-related, respectively, the above equation can be given with the corresponding specific terms.

$$W_f = w_e L t + \beta w_p L^2 t \tag{2}$$

$$w_f = w_e + \beta w_p L \tag{3}$$

where t is the specimen thickness and β is the shape factor related to the form of the plastic zone.

Equation 3 serves for the data reduction. The specific work of fracture (w_f) is determined by the multispecimen approach, i.e. performing the tests on cracked specimens with different ligaments. According to the resistance curve approximation w_e represents the resistance to crack initiation, whereas βw_p the resistance to crack growth. As mentioned before, EWF works under plane stress conditions and thus only in a given ligament range[1-3].

A large body of works addressed the EWF toughness determination of polymers, polymer blends and composites both under static and dynamic conditions[1-2]. The recent vivid development with thermoplastic nanocomposites triggered interest for their toughness

determination. The toughness of thermoplastic nanocomposites is topic of disputes. Many papers concluded toughness improvement, and as many, the opposite owing to incorporation of nanofillers. To shed light on this issue the toughness should be determined by fracture mechanical methods because only their outcome is an inherent material parameter that may be used for comparison purpose. The EWF concept has already been adapted to thermoplastic nanocomposites. Bureau et al.[4] incorporated organophilic montmorillonite in polypropylene (PP) in absence and presence of maleic anhydride grafted PP as coupling agent. Their results are questionable, however, because the *F-x* curves did not meet the self-similarity criterion, which is the essential prerequisite of the applicability of the EWF, as concluded in Ref. 1. Satapathy et al.[5] prepared PP nanocomposites with different carbon nanotube content. Using the EWF these authors tried to find that nanocomposite composition where the ductile-to-semiductile transition appears. However, the accuracy of their EWF results is questionable because the registered *F-x* curves do hardly overlap by a simple linear transformation (i.e. self similarity is blurred). Saminathan et al.[6] made their EWF investigations on clay filled PP and examined the effect of the clay content. One could observe that by increasing filler content the self-similarity of the *F-x* curves gradually disappeared. By contrast, the group of Pegoretti[7] demonstrated that silica and synthetic boehmite alumina (BA) nanofiller containing linear low density polyethylene (LLDPE) the EWF approach works properly. The related *F-x* curves were self-similar and even one could distinguish between yielding (blunting) and necking. This kind of partitioning is a very straightforward tool to extend the application of the EWF for polymers with limited ductility[3]. Unfortunately, a clear splitting between yielding and necking/tearing is quite seldom. Instead of full ligament yielding prior to crack growth with necking, these two processes are usually superimposed.

In order to study the change in the toughness of nanocomposites as a function of nanofillers loading such polymers should be selected which fully meet the EWF's application criteria in their unfilled forms. The latter means full ligament yielding prior to necking and self-similar *F-x* curves in the ligament range investigated. Self-similarity means that the *F-x* curves can be made overlapping by linear transformation. EWF suitable polymers are apart of LLDPE, ethylene-propylene block copolymers (EPBC)[8-9], poly(ε-caprolactone)[10-11], and especially amorphous copolyesters[3,12-14]. Our preliminary investigations along with the learning from the literature suggested that the nanofillers have to be carefully selected, too. Those which have low aspect ratio and can well be dispersed through melt compounding should be favored. This criterion meets by BA[15].

This work was aimed of studying the EWF behavior of EPBC-BA nanocomposites as a function of the BA content. Note that the latter affects the dispersion of the nanofiller because increasing nanofiller content is usually accompanied with prominent agglomeration.

Experimantal

Materials

As matrix material poly(propylene-block-ethylene) (EPBC; Tipplen K499, TVK Nyrt., Tiszaújváros, Hungary) was chosen. This polymer fulfills the most important EWF requirement, namely full ligament yielding prior to crack growth. 5.5-7.5 wt.% acetic acid surface modified water dispersible alumina hydrate (AlO(OH)), boehmite; BA; Disperal P3; Sasol GmbH, Hamburg, Germany) was selected as nanofiller. The average crystallite size of the Disperal P3 nanoparticles was <4.5 nm.

Nanocomposite preparation

Different amounts of nanoparticles (0.5; 1.0; 2.5; 5.0 wt.%) were introduced into the EPBC matrix via extrusion melt compounding in a Labtech Scientific type twin-screw extruder (L/D=44; D=26 mm). The temperature of the extruder zones were 170; 180; 180; 185; 190; 190; 195; 195; 200; 200°C, respectively. The extruded wire was granulated into ca. 3 mm length pieces. The granulated nanocomposites were compression molded into 150x150x0.5mm large sheets with the aid of a Collin Teach-Line Platen Press 200E type hot-press. The sheets were molded at 190°C (kept for 5 min) and 100 bar.

Testing

The BA dispersion was studied in transmission electron microscopy (TEM). The related device (Zeiss LEO 912 Omega, Zeiss Oberkochen, Germany) operated at acceleration voltage of 120 kV. Thin specimens (thickness of about 50 nm), prepared by cryocutting, were subjected to TEM investigations.

Dumbbell type specimens (cross-section of 5.0x0.5 mm) were cut for tensile tests that were carried out on a Zwick Z005 (Ulm, Germany) universal loading machine according to EN ISO 527-1. The testing speed was 2 mm/min and the gauge length was 50 mm.

EWF tests were performed on deeply double edge notched tensile loaded (DEN-T) specimens under quasistatic loading conditions. DEN-T specimens with the dimension 35x70 mm (width x length) were subjected to quasi-static loading at 2 mm/min deformation rate at room temperature. The ligament range covered L=5 to 25 mm. At each ligament 5 specimens

were tested. During the data reduction the energy partitioning method, recommended by Karger-Kocsis[1,3] was used:

$$w_f = w_{f,y} + w_{f,n} = \left(w_{e,y} + \beta' w_{p,y} \cdot L\right) + \left(w_{e,n} + \beta'' w_{p,n} \cdot L\right) \quad (4)$$

where y and n subscripts denote the yield- and necking/tearing-related terms.

The failure mode of the specimens was inspected in light (LM; Olympus BX51, Hamburg, Germany) and scanning electron microscopes (SEM; JEOL JSM-6380LA, Tokyo, Japan). The conductivity of the specimens in SEM was ensured by coating with an Au/Pd alloy.

Result and discussion

BA dispersion

Figure 1 shows that the BA particles are very well dispersed in the EPBC matrix, though their small agglomerates are also observable (marked by black arrows). In the pictures the large dark spots represent the elastomer particles (i.e. ethylene-propylene random copolymer) dispersed in the continuous PP matrix (light field). The particle size of the elastomeric phase in EPBC agrees well with literature data[16].

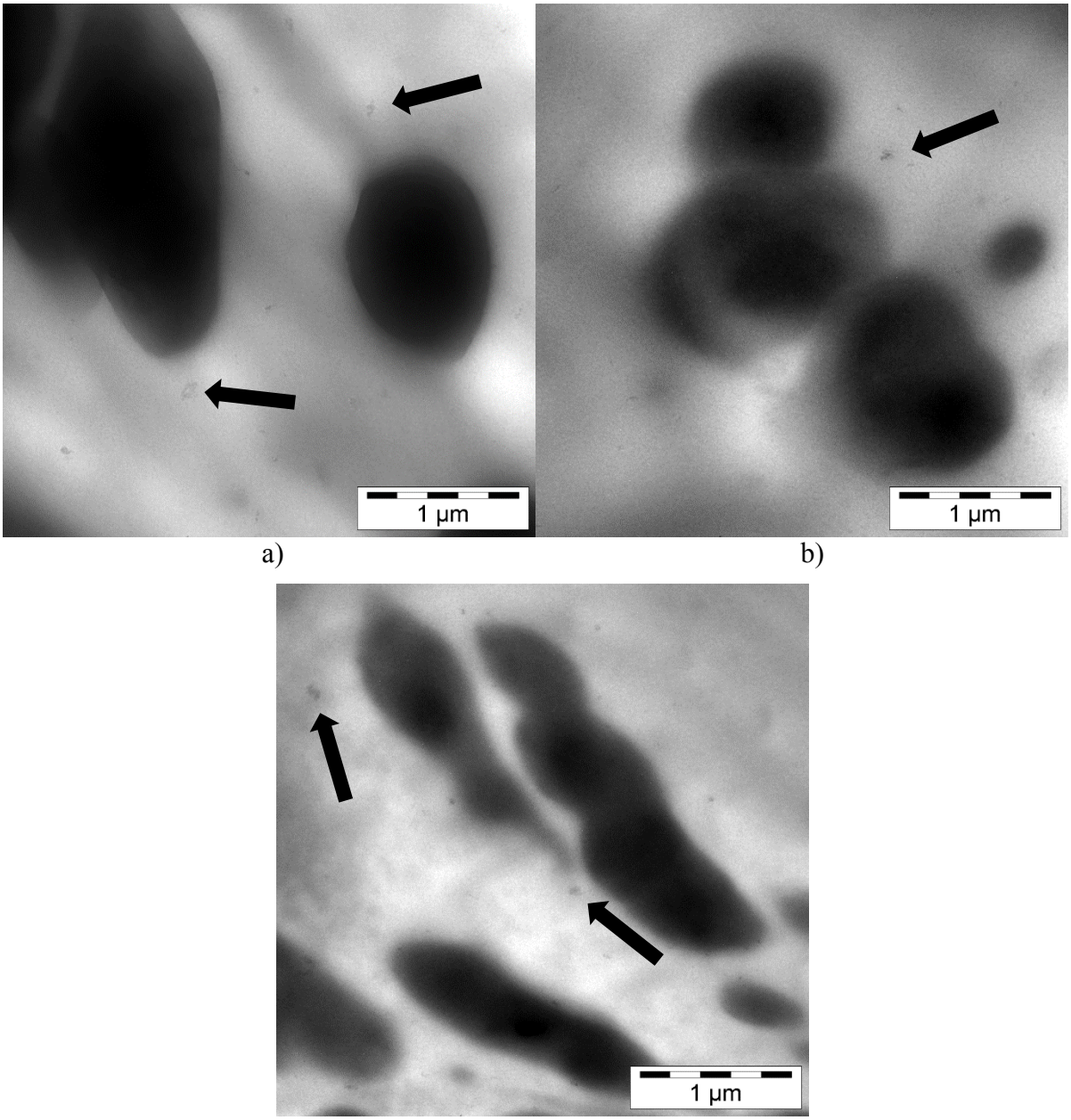

a) b)

c)

Figure 1. TEM micrographs of the EPBC-BA nanocomposites at different BA contents: a) 1.0 wt.%; b) 2.5 wt.%; c) 5.0 wt.%

Figure 2 represents SEM pictures taken from the cryogenic fracture surfaces [(Figure 2(a) and (b)] and from the surface of the DEN-T specimens after the EWF tests [(Figure 2(c) and (d)]. In Figure 2(a) the elastomer particles and the voids remaining after their fall out are indicated by white arrows. The TEM and SEM images in Figures 1 and 2, respectively, confirm the same size range for the dispersed elastomeric phase. At higher magnification well dispersed BA particles are observable [(Figure 2(b)]. Though their size is much larger than the primary crystallite size of BA, Figure 2(b) affirms a very fine, nanoscaled dispersion of the BA nanoparticles in EPBC. SEM image taken from a section of the plastic zone of EPBC-BA-5

(for designation cf. Table I) reveals that also rather big agglomerates are present [(Figure 2(c)]. They serve as stress-concentration sites and induce multiple crazing and shear-yielding in their vicinity [(Figure 2(d)].

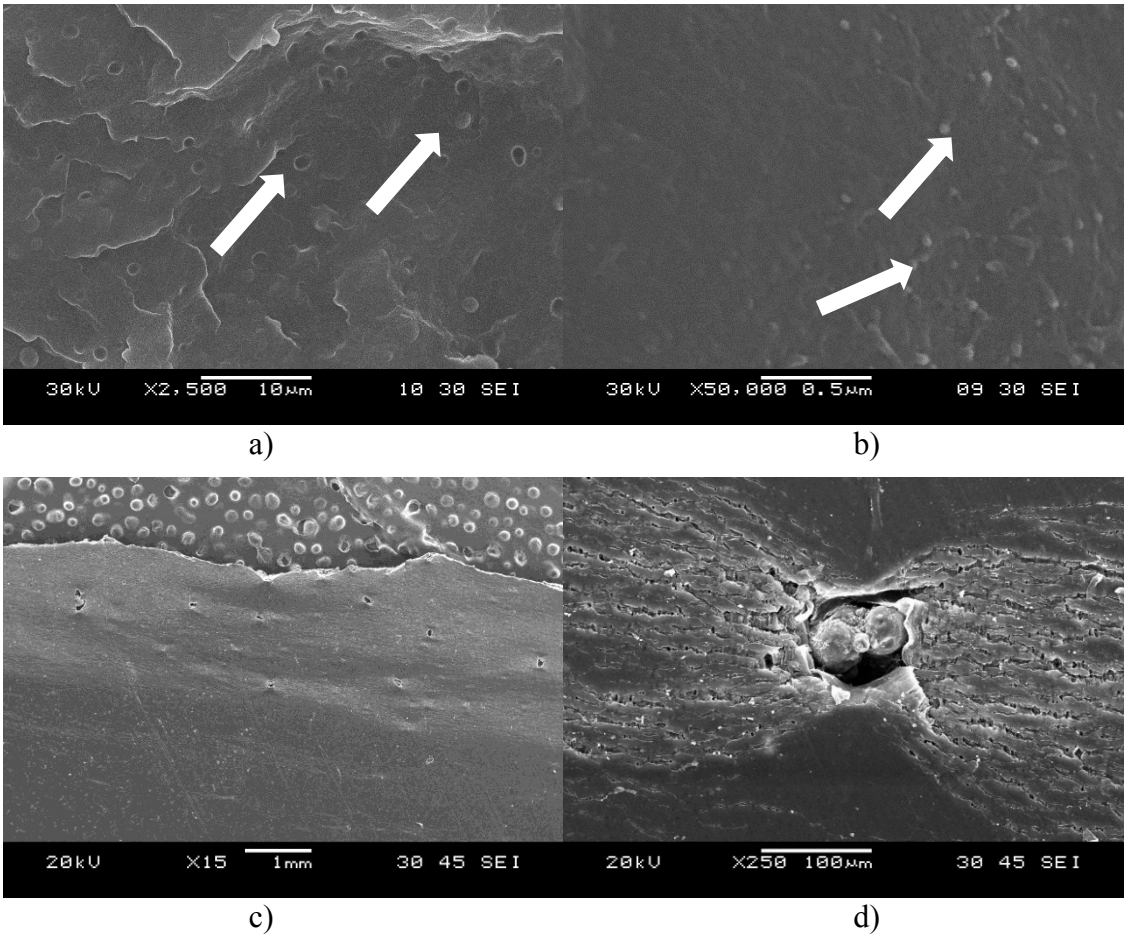

Figure 2. SEM micrographs taken from EPBC-BA nanocomposites: a) cryo-fractured EPBC-BA-1, magnification: 2500x; b) cryo-fractured EPBC-BA-1, magnification: 50000x; c) surface view of fractured DEN-T specimen from the plastic zone of EPBC-BA-5, magnification: 15x; d) surface view of fractured DEN-T specimen from the plastic zone of EPBC-BA-5, magnification: 250x

Tensile characteristics

The E-modulus (E), yield stress (σ_y) and elongation at yield (ε_y) data are tabulated in Table I. One can recognize that BA did not work as reinforcing additive. The E-modulus, σ_y, and ε_y show marginal changes as a function of the BA content. Considering the fact that BA was never reported to hamper the crystallization of the matrix, the missing reinforcing effect is most probably an effect of the BA surface treatment. Further, a portion of the BA particles may be embedded in the elastomeric particles though no direct evidence for that was received from the TEM investigations.

designation	BA content	σ_y	ε_y	E
-	[wt.%]	[MPa]	[%]	[GPa]
EPBC	0.0	22.3 ± 1.1	4.36 ± 0.15	1278 ± 68
EPBC-BA-0.5	0.5	19.8 ± 0.8	4.56 ± 1.65	1180 ± 29
EPBC-BA-1	1.0	20.5 ± 1.2	4.01 ± 0.25	1194 ± 59
EPBC-BA-2.5	2.5	19.8 ± 0.2	3.82 ± 0.12	1211 ± 32
EPBC-BA-5	5.0	20.2 ± 0.4	4.07 ± 0.60	1219 ± 11

Table I. The yield stress, elongation at yield and E-modulus for EPBC and EPBC-BA composites

EWF

Figure 3 compares the characteristic *F-x* curves registered on the DEN-T specimens of the plain EPBC and its BA nanocomposites. The *F-x* traces for EPBC in Figure 3(b) are self-similar, in fact. Yielding is not instantaneous but develops with the time. This is termed sometimes to delayed blunting[17], that can also be resolved in the EPBC-BA nanocomposites. Accordingly, yielding and necking/tearing processes are somewhat superimposed and for their separation only the maximum load may serve. The most striking feature is that the curves deviate markedly from to the expected self-similarly in the necking stage. Because this part represents the crack growth, the course of the corresponding *F-x* section already hints for the inhomogeneous dispersion of the BA nanofiller.

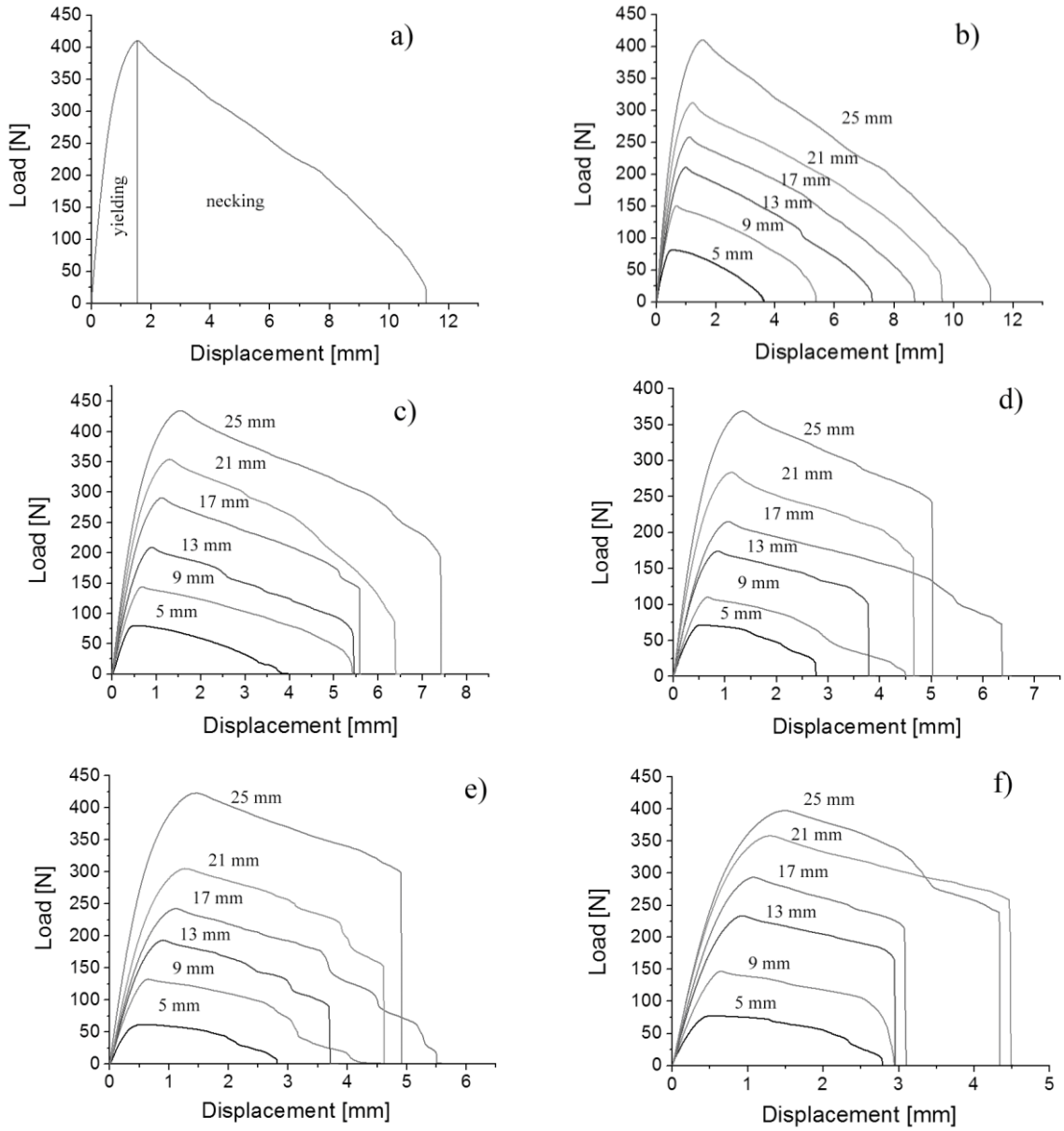

Figure 3. Curve partitioning in principle and selected *F-x* curves of the EPBC-BA nanocomposites, a) splitting between yielding and necking zones,b) EPBC, c) EPBC-BA-0.5, d) EPBC-BA-1, e) EPBC-BA-2.5, f) EPBC-BA-5

Figure 4 depicts the w_f vs. L traces along with the linear regression deduced. The related parameters are tabulated in Table II. Recall that the data in Table II are given with 95% confidence limits.

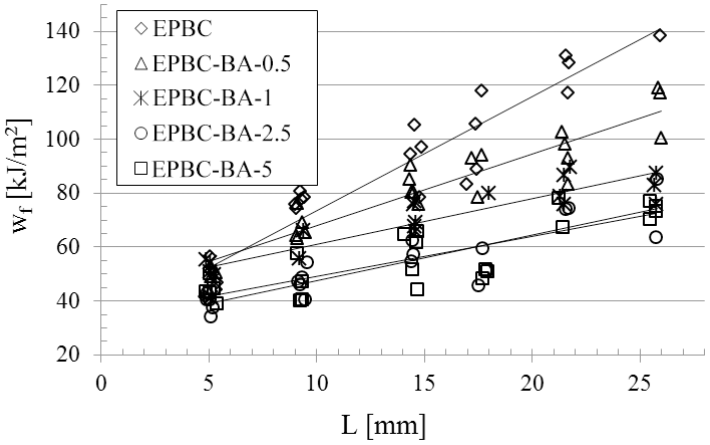

Figure 4. The work of fracture of EPBC and EPBC/BA nanocomposites

Figure 4 along the w_e and βw_p results in Table II demonstrate that w_e goes through a maximum (at about 1 wt.% BA). The w_e values at higher BA contents agree fairly with that of the matrix. βw_p, representing the resistance to crack growth is, however, was decreasing with increasing BA content.

Material	w_e	βw_p	R^2	w_p
-	[kJ/m^2]	[MJ/m^3]	[-]	[MJ/m^3]
EPBC	30.02 ± 4.61	4.32 ± 0.30	0.90	17.30 ± 1.20
EPBC-BA-0.5	41.10 ± 3.72	2.67 ± 0.22	0.87	10.60 ± 0.87
EPBC-BA-1	44.15 ± 3.08	1.68 ± 0.19	0.81	6.38 ± 0.72
EPBC-BA-2.5	30.52 ± 3.31	1.70 ± 0.22	0.75	6.95 ± 0.90
EPBC-BA-5	34.48 ± 3.58	1.47 ± 0.22	0.66	6.79 ± 1.02

Table II. The essential and non-essential (plastic) work of fracture parameters for EPBC and EPBC/BA composites

To determine explicitly the w_p values, the β shape factor has been determined through Equation (5) supposing the presence of an elliptical plastic zone[18]. The half height ($h/2$) of the plastic fracture zone [(Figure 5(a)] has been measured and the β value computed for each tested DEN-T specimen. They were afterward averaged for each composite and w_p calculated. (cf. Table II).

$$\beta = \frac{\pi \cdot h}{4L} \tag{5}$$

It should be noted that for the nanocomposites, especially at higher filler contents, stripes appeared on the border of the outer plastic deformation zone and the surrounding undeformed area. This kind of instability appeared also in the *F-x* curves, resulting waves in the force trace (see Figure 3(e), L=17 mm). This phenomenon is similar to the stress-oscillation behavior at

tensile tests of some thermoplastic materials[19]. The formed wavy borderline is indicated by white arrow in Figure 5(b). These stripes made the characterization of the half height more difficult. To overcome this problem the first dark stripe was chosen as the end of the outer plastic deformation zone [cf. Figure 5(b)].

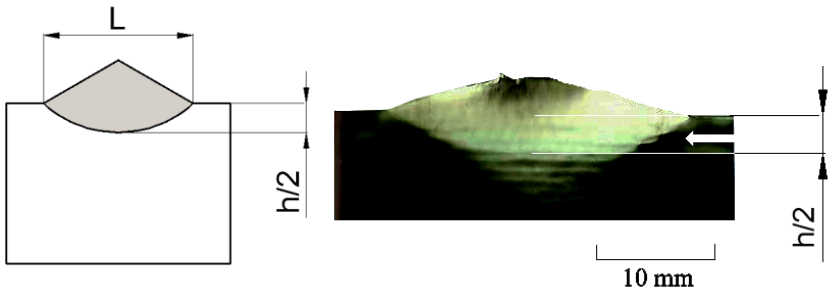

Figure 5. Determination of the β shape factor by measuring the half height of plastic deformation zone: a) plastic deformation zone and measuring of $h/2$ schematically, b) stripes under the plastic zone on a broken DEN-T specimen

Data in Table II indicate that β is decreased with increasing BA content. This was associated with a prominent decrease in w_p. This means that the presence of BA decreased the plastic deformability of the EPBC.

Coming back to Figure 3 attention should be called to the fact that the yielding sections of the *F-x* curves always obey the self-similarly criterion. Therefore we may follow the energy partitioning proposed by Karger-Kocsis[1,3]:

$$w_{f,y} = w_{e,y} + \beta' w_{p,y} L \tag{6}$$

where $w_{f,y}$ is the yielding-related specific work of fracture, $w_{e,y}$ is the yielding-related specific essential work, β' is the yielding-related shape factor, and $w_{p,y}$ is the yielding-related specific plastic work.

The yielding-related EWF data have markedly higher regression coefficients than the "overall" ones - compare data in Tables III and II, respectively. This confirms that the EWF method can be adapted to the yielding-related sections of the *F-x* curves of ductile polymer nanocomposites which show some instability in the subsequent necking/tearing sections [cf. Figure 3(c) to (f)].

Material	$w_{e,y}$	$\beta' w_{p,y}$	R^2
-	[kJ/m^2]	[MJ/m^3]	[-]
EPBC	2.93 ± 0.26	0.75 ± 0.02	0.990
EPBC-BA-0.5	2.97 ± 0.56	0.75 ± 0.03	0.975
EPBC-BA-1	2.89 ± 0.44	0.71 ± 0.02	0.974
EPBC-BA-2.5	2.60 ± 0.56	0.65 ± 0.03	0.949
EPBC-BA-5	2.77 ± 0.47	0.66 ± 0.03	0.957

Table III. The yielding related EWF parameters for EPBC and EPBC/BA composites

Considering the scatter in the $w_{e,y}$ data one can conclude that BA does not effect this value in the studied BA nanofiller range. It should be noted the $w_{e,y}$ is argued to be closely matched with the plane-strain essential work of fracture[3,20]. If this assumption is correct than the BA nanofiller did not affect the toughness of the EPBC matrix which is rather peculiar. The $\beta' w_{p,y}$ term decreased with increasing BA content, similar to βw_p.

The question arises whether or not there is a correlation between the yielding-related tensile and yielding related EWF results. Plotting $w_{e,y}$ and $\beta' w_{p,y}$ as a function of $\sigma_y \varepsilon_y$ fairly linear correlations are obtained [Figure 6(a) and (b)].

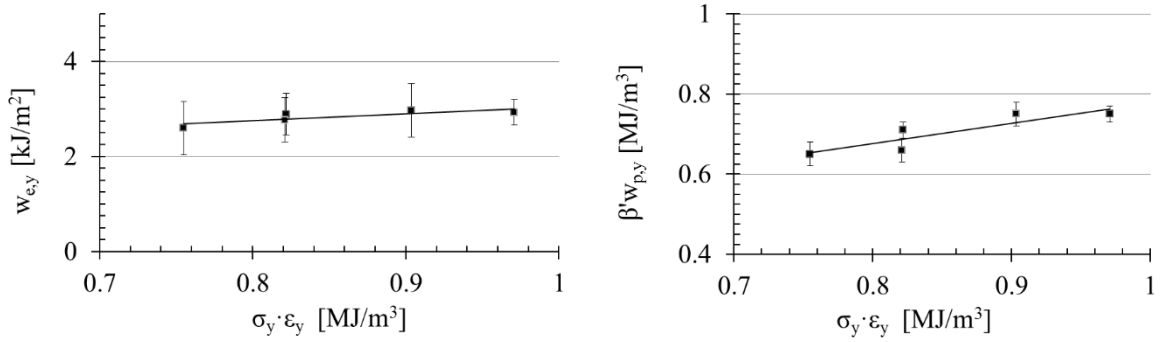

a) b)

Figure 6. Yielding-related specific essential ($w_{e,y}$; a) and non-essential work of fracture terms ($\beta' w_{p,y}$, b) as a function of $\sigma_y \varepsilon_y$

Failure

Macrophotographs taken from the plastic zones of the DEN-T specimens of EPBC and its nanocomposites are displayed in Figure 7. It can be clearly seen that the height of the plastic zone decreases with increasing BA content. Recall that this is implicitly given by the data in Table II. Figure 7 reassures that the shape of the plastic zone was an ellipse, in fact. The stress

whitening in the plastic zone is due to voiding and crazing phenomena. The fracture surface of the nanocomposites with higher BA content is zig-zag type. This is the macroscopic appearance of the inhomogeneous dispersion the BA nanoparticles.

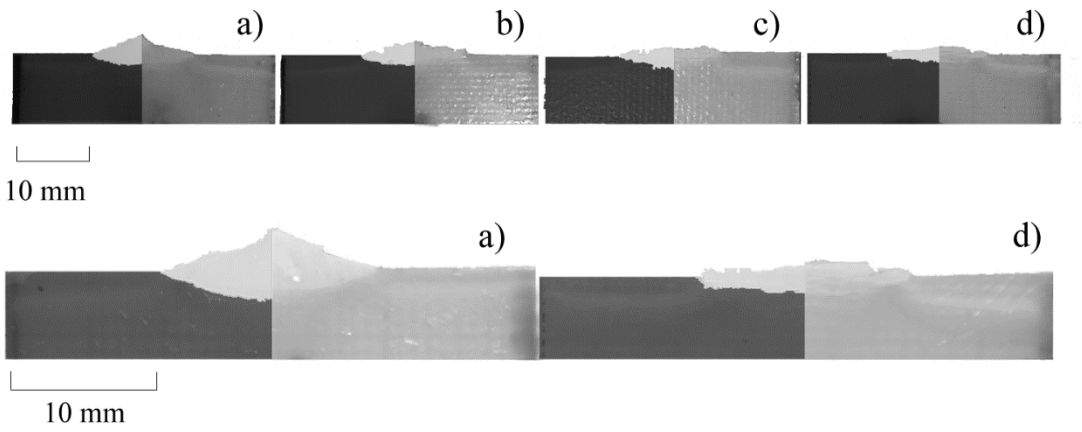

Figure 7. LM pictures on selected DEN-T specimens at the same ligament length (L=13mm) for a) EPBC, b) EPBC-BA-1, c) EPBC-BA-2.5, d) EPBC-BA-5. Note that the composed picture show the same plastic zone in contrasted (image processing) and original forms (left and right sides, respectively)

SEM pictures taken from the fracture process zone of EPBC shows ductile failure that occurred after voiding/crazing via exhaustive fibrillation[21]. This feature, though less prominent with increasing BA content, is characteristic for all nanocomposites. It is demonstrated on examples of EPBC-BA-1 [(Figure 8(a)] and EPBC-BA-5 [(Figure 8(b)]. SEM pictures taken from the fracture surfaces of the nanocomposites evidence that the agglomerated BA particles act as stress concentrators and induce voiding [(Figure 8(c)]. Small matrix ligaments between the voids are torn plastically. Large agglomerates cause secondary cracking phenomena. In this case voiding starts below the final fracture surface. Larger ligaments between the stress concentrating agglomerates and related voids undergo semiductile deformation. These events are responsible for the unstable necking observed in the *F-x* traces [cf. Figure 3(c) to (f)].

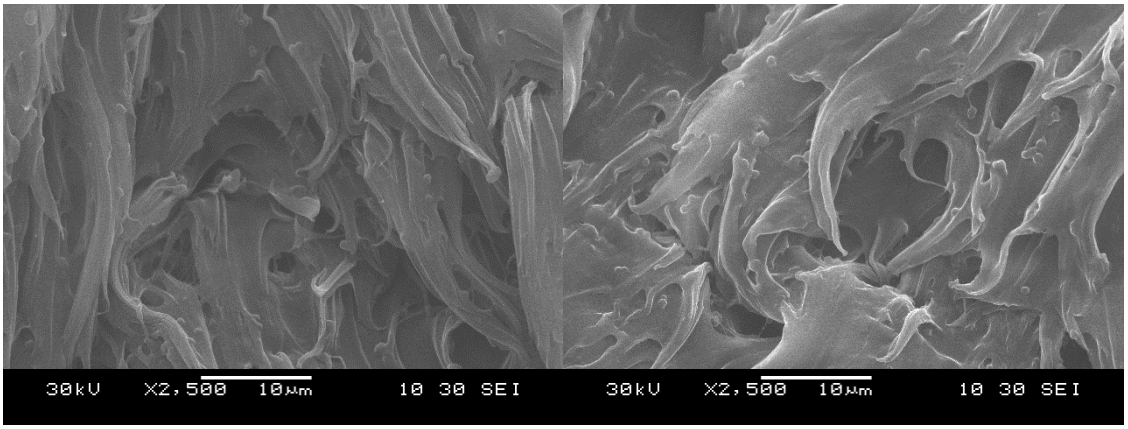

a) b)

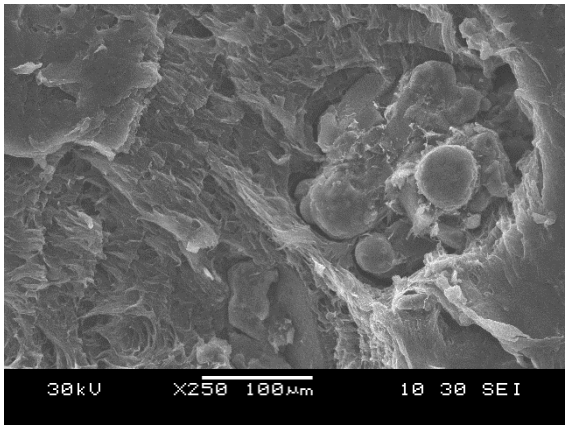

c)

Figure 8. a) fracture surface of the DEN-T specimen of EPBC-BA-1, magnification: 2500x; b) fracture surface of the DEN-T specimen of EPBC-BA-5, magnification: 2500x; c) 5 fracture surface of the DEN-T specimen of EPBC-BA-5, magnification: 250x

Conclusion

Based on this work devoted to study the toughness of EPBC containing up to 5 wt.% BA nanofiller using the EWF concept, the following conditions can be drawn:

- nanofillers' dispersion and content have a great impact on the necking section of the force-displacement curves. This may disqualify the EWF method for the toughness assessment
- reliable EWF parameters can only be derived by considering the yielding section of the force-displacement curves. The related EWF parameters correlated with the product of the yield stress and yield strain from tensile tests,
- the applied BA nanoparticles did not act as reinforcement. Nevertheless, in a given range it enhanced the resistance to crack initiation. BA supported the voiding via which the resistance to crack growth has been reduced.

Acknowledgement

This work was performed in the framework of a bilateral cooperation agreement between Italy and Hungary (HU11MO8 and TÉT-10-1-2011-0218, respectively). This work is also connected to the scientific program of the "Development of quality-oriented and harmonized R+D+I strategy and functional model at BME" project. This project is supported by the New Széchenyi Plan (Project ID: TÁMOP-4.2.1/B-09/1/KMR-2010-0002).

References

1. Bárány, T.; Czigány, T.; Karger-Kocsis, J. *Prog. Polym. Sci.* **2010**, *35*, 1257-1287.
2. Martínez, A. B.; Gámez-Pérez, J.; Sánchez-Soto, M.; Velasco, J. I.; Santana, O. O.; Maspoch, M. Ll. *Eng. Fract. Mech*. **2009**, *16*, 2604-2617.
3. Karger-Kocsis, J. *Polym. Bull*. **1996**, *37*, 119-126.
4. Bureau, M. N.; Perrin-Sarazin, F.; Ton-That, M-T. *Polym. Eng. Sci.* **2004**, *44*, 1142–1151.
5. Satapathy, K.; Ganß, M.; Weidisch, R.; Pötschke, P.; Jehnichen, D.; Keller, T.; Jandt, K. D. *Macromol. Rapid Comm.* **2008**, *28*, 834-841.
6. Saminathan, K.; Selvakumar, P.; Bhatnagar, N. *Polym. Test.* **2008**, *27,* 296-307.
7. Pedrazzoli, D.; Ceccato, R.; Karger-Kocsis, J.; Pegoretti, A. *Express Polym. Lett.* **2013**, *7*, 652-666.
8. Maspoch,M. L. l.; Gámez-Pérez, J.; Gordillo, A.; Sánchez-Soto, M.; Velasco, J. I. *Polymer* **2002,** *43,* 4177-4183.
9. Martínez, A. B.; Segovia, A.; Gamez-Perez, J.; Maspoch, M. L. l. *Eng. Fract. Mech*. **2010,** *77,* 2654-2661.
10. Tuba, F.; Khumalo, V. M.; Karger-Kocsis, J. *J. Appl. Polym. Sci*. **2013**, *129*, 2950-2958.
11. Tuba, F; Oláh, L.; Nagy, P. *J.App. Polym. Sci.* **2011,** *120*, 2587-2595.
12. Karger-Kocsis, J.; Bárány, T.; Moskala, E. J. *Polymer* **2003,** *44,* 5691-5699.
13. Chen, H.; Karger-Kocsis, J.; Wu, J. *Polymer* **2004**, *45*, 6375-6382.
14. Poon, W. K. Y.; Ching, E. C. Y.; Cheng, C. Y.; Li, R. K. Y. *Polym. Test.***2001,** *20,* 395-401.
15. Karger-Kocsis, J.; Khumalo, V. M.; Bárány, T.; Mészáros, L.; Pegoretti, A. *Compos. Interface.* **2013,** *20*, 395-404.
16. Karger-Kocsis, J. Polypropylene Structure, blends and composites 2; Chapman & Hall: London, **1995**; Vol. 2, Copolymers and blends
17. Karger-Kocsis, J.; Bárány, T. *Polym. Eng. Sci.* **2002,** *42,* 1410-1419.
18. Karger-Kocsis J., Czigány, T. *Polymer* **1996,** *37,* 2433-2438.
19. Vas, L. M.; Ronkay, F.; Czigány, T. *Express Polym. Lett.* **2009,** *3,* 63-69.
20. Ferrer Balas, D., Maspoch, M. Ml., Martinez, O. O. *Polym. Bull.* **1999,** *42,* 101-108.
21. Michler, G. H., Balta-Calleja, F., J. Nano- and Micro Mechanics of Polymers; Carl Hanser Verlag: Munich, **2012.**